Journal of Physical Science, Vol. 33(2), 1–17, 2022

RF Sputtered ZnO Nanoballs on Porous Substrate for Highly Sensitive NO_2 Gas Sensing Applications

Pankaj Varshney,[1] Vinay Kumar,[2,3] Pankaj Singh,[4] Ramphal Sharma[5] and Arvind Kumar[6*]

[1]Department of Physics, SRM Institute of Science and Technology,
Delhi-NCR Campus, Ghaziabad 201204, India
[2]Centre for Bio-nanotechnology, Chaudhary Charan Singh,
Haryana Agriculture University, Hisar 125004, India
[3]Department of Physics, Chaudhary Charan Singh, Haryana Agriculture University,
Hisar 125004, India
[4]Department of Physics, Deshbandhu College, University of Delhi, Delhi 110019, India
[5]Thin Film and Nanotechnology laboratory, Department of Physics,
Dr. Babasaheb Ambedkar Marathawada University,
Aurangabad 431004, India
[6]Thin Film Laboratory, Department of Physics, Indian Institute of Technology Delhi,
Delhi 110016, India

[*]Corresponding author: arvindphysics008@gmail.com

Published online: 25 August 2022

To cite this article: Varshney, P. et al. (2022). RF sputtered ZnO nanoballs on porous substrate for highly sensitive NO_2 gas sensing applications. *J. Phys. Sci.*, 33(2), 1–17. https://doi.org/10.21315/jps2022.33.2.1

To link to this article: https://doi.org/10.21315/jps2022.33.2.1

ABSTRACT: *In this work, zinc oxide (ZnO) nanoballs were directly deposited on porous silicon (PS) substrates using RF magnetron sputtering method. The PS substrates were synthesised at room temperature via metal assisted chemical etching technique. The structural, surface morphological and cross-sectional properties of as prepared ZnO nanoballs were investigated by x-ray diffraction, Raman spectroscopy and field emission scanning electron microscopy techniques, respectively. The interaction of nitrogen dioxide (NO_2) gas molecules with sensing layer and all sensing properties under lower detection limit (2 ppm–100 ppm) were studied in detail. The proposed ZnO nanoballs sensor chip exhibits high sensing response (29.2%) with fast response/recovery times (70 sec/96 sec) to 20 ppm NO_2 in dry air at 250°C. Thus, the findings recommend the viability of ZnO nanoballs sensor as highly sensitive and selective NO_2 gas sensor at moderate operating temperature regime.*

Keywords: zinc oxide, nanoballs, porous silicon, nitrogen dioxide, sensor

1. INTRODUCTION

In the present time, our environment has become highly poisonous due to human activities and carelessness towards pollution control.[1] Rapid industrial development along with improving life quality caused to increase the percentage of toxic gases in the environment. The rising portion of greenhouse gases by burning of fossil fuels in our atmosphere caused climate change globally.[2,3] Various toxic gases such as ammonia (NH_3), carbon monoxide (CO), Nitrogen monoxide (NO) and Nitrogen dioxide (NO_2) possess enormous health issues in front of human beings. Among these gases, NO_2 is the most hazardous air pollutant causing lungs, respiratory and cardiovascular disease even at low concentration. The threshold limit value (TVL) for NO_2 is 3 ppm for continuous exposure of 8 h or detached exposure of 40 h in a week at the workplace without known adverse effects. Moreover, the ceiling limit (CL) for NO_2 is 5 ppm which is the concentration that should not exceed at any time in the environment.[4] Therefore, the precise detection of ppm level NO_2 along with the development of high-performance sensor are required for the protection of human health and to maintain the quality of the environment. In the present scenario, low cost and environment friendly sensors are highly desirable to detect hazardous gases which are capable to operate near room temperature and consume minimum electric power.[5] Nowadays, numerous synthesis techniques have been used to fabricate environmental gas sensors. Several materials such as metal oxides,[6,7] graphene and its compounds,[8] metal sulfides,[9] etc. are also being incorporated into sensor technology to meet the present requirements. Among these materials, metal oxide semiconductors are broadly employed as sensing element due to their low cost, highly stable, nontoxic in nature and repeatable over time.[10,11] However, this kind of sensors possess some demerits such as lack of selectivity towards specific gas and worked at relatively high operating temperatures.

Nanostructured metal oxides provide enhanced sensing properties due to their high surface to volume ratio and hence increase the active surface area of sensing element for the interaction of analyte gas molecules over the surface. In sensor technology, doping with catalyst, fabrication of heterojunction, illuminating sensor surface and decoration of metal nanoparticles over sensing element are other methods to enhance the sensor performance. In addition, particular morphologies of metal oxides such as nanorods, nanospheres, nanoballs, nanosheets are also reported and exhibit enhanced sensor response with high selectivity towards specific gas. In the present work, we are using porous silicon substrates to develop hydrophobic surface and hence to minimise the humidity effect on the sensor performance. Porous nanostructures will provide high

active surface area and high diffusivity to analyte gas molecules to enhance the sensor performance at relatively low operating temperatures.[12]

Metal oxide semiconductors such as zinc oxide (ZnO), titanium dioxide (TiO_2), cerium(IV) oxide (CeO_2), gadolinium(III) oxide (Gd_2O_3), iron(III) oxide (Fe_2O_3), etc.[13–16] have been widely investigated for sensor applications. However, ZnO nanostructures-based sensors have attracted much attention due to their excellent electrical and optical properties. It is non-toxic, less corrosive, highly stable and easily synthesised which is effectively used in gas sensor devices as well as in other energy applications.[17,18] Different nano structured morphologies of the ZnO can be easily synthesised by several techniques such as DC/RF sputtering, pulsed laser deposition, hydrothermal, sol gel, chemical vapour growth, etc.

In this work, ZnO nanospheres were synthesised on porous silicon (PSi) substrates by RF sputtering method at room temperature. The NO_2 gas sensing properties of ZnO/PSi sensor element were examined in detail. The nanospheres of ZnO showed the improved response towards NO_2 under lower detection limit down to 2 ppm. Herein, a study on gas selectivity and reproducibility along with sensing mechanism were also discussed in detail. Moreover, we have also studied the changes in sensing performance under different humidity conditions for practical applications.

2. EXPERIMENTAL DETAILS

2.1 Materials and chemicals

The zinc (Zn) target of 5 mm in thickness and 50.4 mm in diameter with high purity (99.98%) was purchased from ACI Alloys Inc. USA. Argon (Ar) and oxygen (O_2) gas cylinders were obtained from Sigma Gases, New Delhi, India. N-type Si (111) substrates were bought from Excel Instruments, Mumbai, India.

2.2 Sensor fabrication

In this work, to synthesise the PSi substrates, n-type highly doped and (111) oriented silicon substrates with resistivity of 0.05 Ω-cm–0.07 Ω-cm were used. These silicon substrates were ultra-sonicated first in isopropyl alcohol and later in acetone consecutively for 10 min each. The prepared porous silicon (Si) substrates were also cleaned in deionised (DI) water and then immersed in piranha solution which contains sulfuric acid (H_2SO_4) 30% and hydrogen peroxide (H_2O_2) 90% for a period of 15 min in volume ratio of 3:1.

This solution was prone to all the organic species and established a thin oxide layer over the surface. It is then detached at room temperature by etching in 2% aqueous Hydrofluoric (HF) solution for 8 min. Thereafter, Si wafers were washed out with aqueous 4% HF to detach native oxide layer present on the surface and cleaned them in DI water and dried up with Ar gas flow for few minutes. The schematic representation of all steps used during formation of PSi substrate is shown in Figure 1.

Herein, ZnO nanoballs were grown on the as prepared PSi substrate using RF magnetron sputtering method. During sputtering, atom by atom deposition takes place to fill the pores of 900 nm in diameter and we get nanoballs like surface morphology. Nanoballs like structure possess high active surface area for the interaction of analyte gas molecules over the sensor surface, caused to enhance the sensing properties.

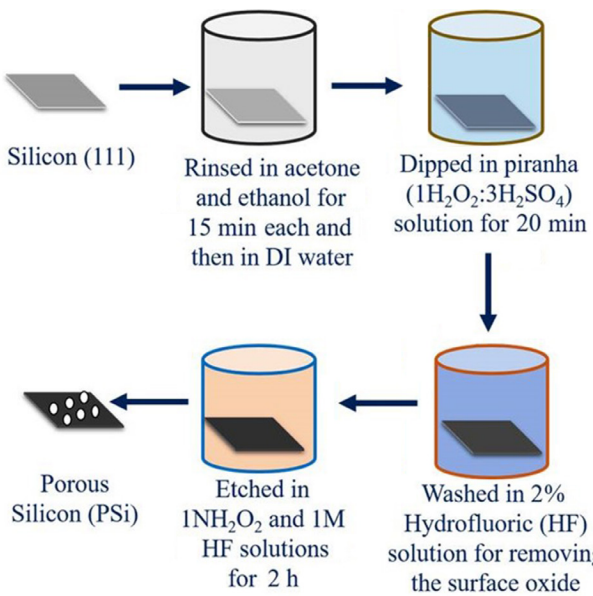

Figure 1: Schematic diagram for the synthesis of porous silicon substrates using chemical etching process.

Sputtering is one of the most prominent physical vapour deposition (PVD) technique to fill the pores of even 100 nm in diameter at room temperature. Moreover, using sputtering we can also synthesise the high-quality contamination free thin films in wide range of operating temperature. Prior to deposition, to obtain high quality thin film, the base pressure of sputtering chamber was achieved 5×10^{-6} Torr using turbo molecular pump backed by rotary pump.

To initiate the plasma, 20 sccm Ar gas was inserted into the deposition chamber using mass flow controller. Here, ZnO nanoballs thin film samples were synthesised using Zn sputtering target. During deposition, the Ar:O_2 gas ratio of 4:1 was maintained thoroughly using mass flow controller. The distance of 7 cm between target and substrate was fixed to fill the Si pores at room temperature. The sputtering power of 60 watt was used at fixed working pressure of 5 mTorr. Four ZnO thin film samples with various thicknesses of 0.4 μm, 0.9 μm, 1.5 μm and 2.2 μm were synthesised using sputtering. The thickness of each ZnO thin film sample was controlled by deposition time. To synthesise the ZnO nanoballs, the deposition time was fixed to 1 h at room temperature.

2.3 Characterisation

The crystallographic structure of the ZnO layer was studied using x-ray diffractometer (CuK_{α} radiation, 1.5406 Å) with a scan rate of 2°/min at room temperature. The chemical bonding and structural analysis of as prepared sample was investigated by Raman spectroscopy (Renishaw, United Kingdom) with 514 nm laser as an excitation wavelength. The surface morphology and cross-sectional measurements of ZnO layer were performed using field emission scanning electron microscopy (FESEM, Carl Zeiss Ultra Plus). I-V curve and gas sensing properties of proposed sensor were examined using Keithley source meter connected with personal computer.

The gas sensing setup comprises of a steel chamber of volume 200 cm^3. It is equipped with mass flow controller to monitor the flow of different gases and an electric heater to precisely measure the operating temperatures. For gas sensing and I-V measurements, silver paste was used to form the electrical contacts on the top surface of sensing layer. During sensing measurements, we measured the base line resistance in dry air at fixed flow rate of 2 standard L per min (slpm) at working temperature of 250°C. Thereafter, the mixture of high purity NO_2 gas and dry air was inserted into the testing chamber at a fixed rate of 2 slpm using mass flow controller under different humidity conditions. Thereafter, we used different gases mixed in dry air and inserted into the test chamber one by one with controlled flow rate using mass flow controller.

3. RESULTS AND DISCUSSION

3.1 Structural properties

Figure 2(a) shows the x-ray diffraction (XRD) pattern of ZnO thin film deposited on PS substrate. It depicts four characteristic peaks centred at 2θ equal to

31.82°, 34.56°, 36.45° and 56.88°, respectively, which corresponds to 100, 002, 101 and 110 orientations of hexagonal wurtzite structure of ZnO [JCPDS card no. 80-0075]. The XRD reflection observed at 69.84° corresponds to 111 orientation of porous silicon substrate (JCPDS no. 271402).

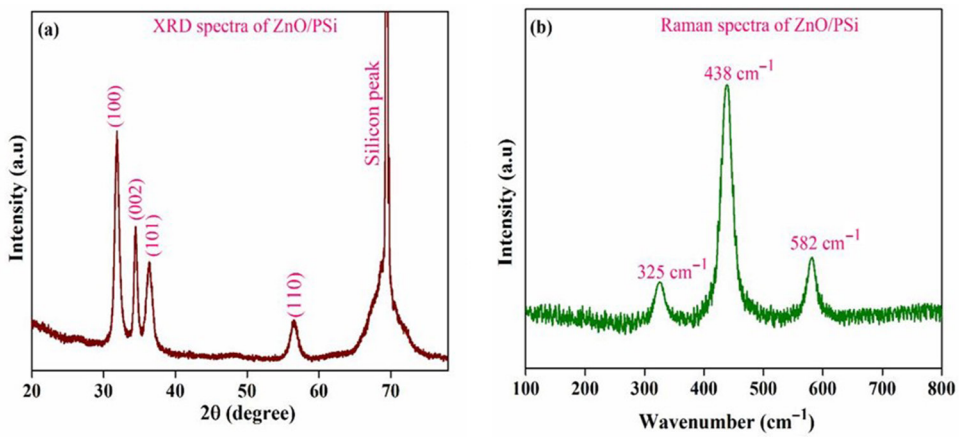

Figure 2: (a) X-ray diffraction and (b) Raman spectra of ZnO/PSi thin film sample.

The crystallite size (d), inter-planar distance (l), dislocation density (δ), number of crystallite size per unit area (n) and distortion parameters (z) were calculated using the following equations[19]:

$$d = \frac{0.9\,\lambda}{\beta \cos\theta} \tag{1}$$

$$l = \frac{\lambda}{2 \sin\theta} \tag{2}$$

$$\delta = \frac{1}{d^2} \tag{3}$$

$$n = \frac{1}{d^3} \tag{4}$$

$$z = \frac{\beta}{\tan\theta} \tag{5}$$

Using XRD curve all the calculated parameters for ZnO thin film are shown in Table 1.

Table 1: XRD parameters of ZnO thin film.

2θ (degree)	βcosθ in radian	d in (nm)	δ ($m^{-2}\times10^{15}$)	l (Å)	n ($m^{-2}\times10^{14}$)	z
31.82	0.01290	10.74	8.669	2.8100	2.268	0.04708
34.56	0.01105	12.00	6.944	2.5932	1.500	0.03536
36.45	0.01425	9.70	10.628	2.4636	2.699	0.04557
56.88	0.02058	6.80	21.626	1.6174	5.142	0.04314

From Equation (1), the average crystallite size was found to be 9.8 nm (as shown in Table 1). Moreover, the Williamson-Hall plot for ZnO thin film is shown in Figure S1. It can be seen that the average crystallite size was found to be 12.24 nm and the micro strain in the ZnO film was observed to be 0.01063.

A Raman spectrum of deposited ZnO thin film is shown in Figure 2(b). It exhibits three characteristic peaks centred at 325 cm^{-1}, 438 cm^{-1} and 582 cm^{-1}. The Raman peak observed at 325 cm^{-1} is second order spectral feature, which basically originates from zone boundary phonons of ZnO and it is associated with A_1 mode of transverse optical (TO).[20] The Raman active phonon modes found at 438 cm^{-1} and 582 cm^{-1} collaborated to E_2 high mode and E_1 longitudinal optical (LO) vibration modes of first order, respectively.[21] Both these vibrational modes indicate the hexagonal structure with good quality of ZnO crystal, which is consistent with XRD results. Thus, these structural measurements reveal that the sensing layer is made up of pure ZnO material.

Figures 3(a) and (b) show the FE-SEM surface morphologies of PSi substrate and as synthesised ZnO layer on PSi, respectively. As shown in Figure 3(a), the average pore diameter was found to be 900 nm. Figure 3(b) reveals the densely packed nanoballs (NBs) like morphology of ZnO thin film. It also depicts that the average size of ZnO nanoballs was observed to be 800 nm. Figure 3(c) exhibits the cross-sectional view of PSi substrate, which indicates the vertical depth of the pores is about 1 micron (μm). Figure 3(d) shows the cross-section cut of ZnO coated PSi sensing element. It can be seen that the thickness of ZnO layer is about 1.5 μm. We also performed the energy dispersive spectrometry (EDS) mapping of as prepared ZnO thin film (as shown in Figure S2). Herein, Zn and O_2 elements are uniformly distributed over the surface of the sensing element.

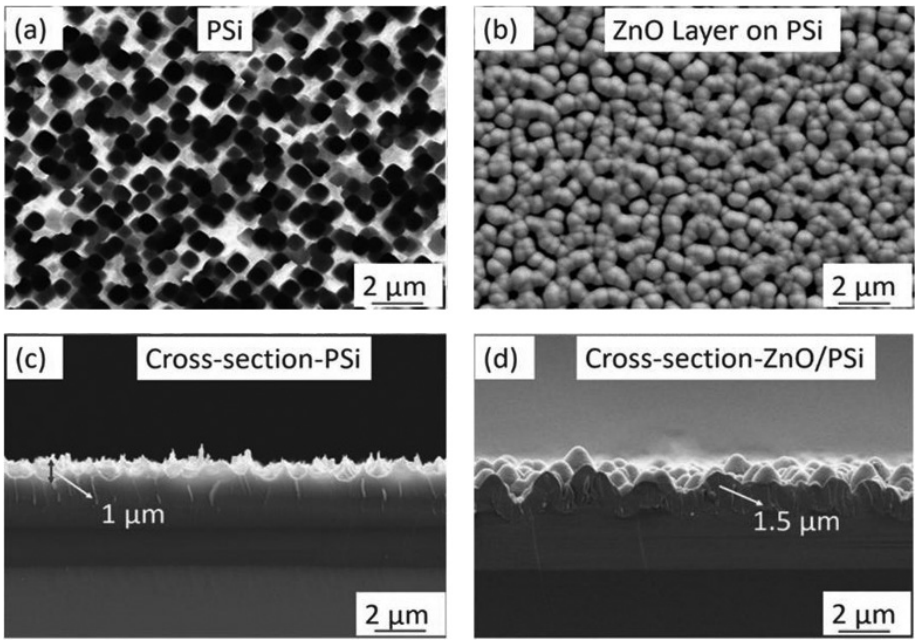

Figure 3: (a) FE-SEM image of PSi, (b) FE-SEM image of ZnO/PSi thin film sample, (c) cross-section cut of PSi and (d) cross-section cut of ZnO/PSi thin film sample.

Hydrophobic surface shows water-repellent property, so that the water droplets which are residing on sensor surface exhibit contact angle greater than 90°.[22] Figures 4(a) and (b) show the contact angle image of bare PSi and ZnO coated PSi, respectively. The contact angle values (using sessile drop method) for bare PSi and ZnO coated PSi were found to be 100° (±2°) and 120° (±2°) degree, respectively. It can be seen that the ZnO coated PSi sensor element is highly hydrophobic in nature as compared to bare PSi substrate.

Hydrophobicity measurements of bare PSi and ZnO coated PSi were carried out by calculating the contact angle of a water droplet on top of materials surface at four different places. Herein, the hydrophobic PSi substrate can act as a template for the uniform growth of ZnO nanoballs. The hydrophobic sensor surface caused to decrease the effect of moisture on the device performance, resulting to improve the sensitivity as well as cyclability.

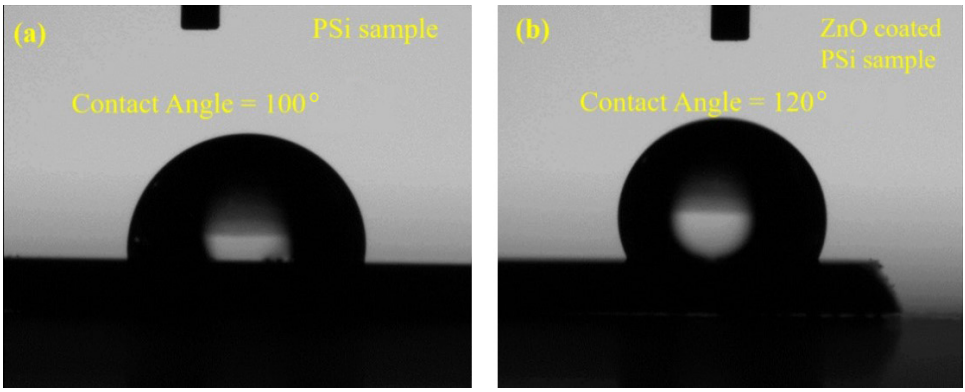

Figure 4: (a) Contact angle image of porous silicon and (b) Contact angle image of ZnO.

3.2 Gas sensing characterisation

The change in electric resistance upon interaction of analyte gas molecules over the sensor surface depends on the type of majority charge carriers present in the material as well as on the nature (reducing or oxidising) of target gas molecules.[23] As it can be observed that the oxidising gases (e.g. NO_2) behave like acceptors, hence increasing the electrical resistance of n-type sensing material and in contrary it decreases the resistance of p-type semiconducting materials.[24] For oxidising gases with n-type sensing element the sensor response is defined by Equation (6) as[25]:

$$\text{Sensor Response (\%)} = \frac{Rg - Ra}{Ra} \times 100 \tag{6}$$

where, *Rg* and *Ra* are the sensor resistance in the presence of oxidising gas and in dry air, respectively.

Figure 5(a) depicts the current-voltage characteristics for ZnO/PSi thin film sample at 250°C in the presence of dry air and 20 ppm NO_2 gas mixed with dry air. It depicts the rectifying diode behaviour of device in dry air as well as in 20 ppm NO_2 gas at 250°C within the voltage range of −3V to 3V. This reveals the change in the electronic properties of sensing layer upon exposure to analyte gas molecules. It can be observed that after exposure to 20 ppm NO_2 the number of free charge carriers on sensor surface increases, which causes to improve the electrical conductivity.[26]

Figure 5(b) shows the sensor response curve at different operating temperatures towards 20 ppm NO_2 with flow rate of 2 slpm in dry air. It can be seen that the sensor device exhibits the increasing trend of sensor response up to operating temperature of 250°C. As we increase the working temperature, the interaction between oxygen ions and analyte gas molecules increases, which can significantly rise the response of the given sensor.

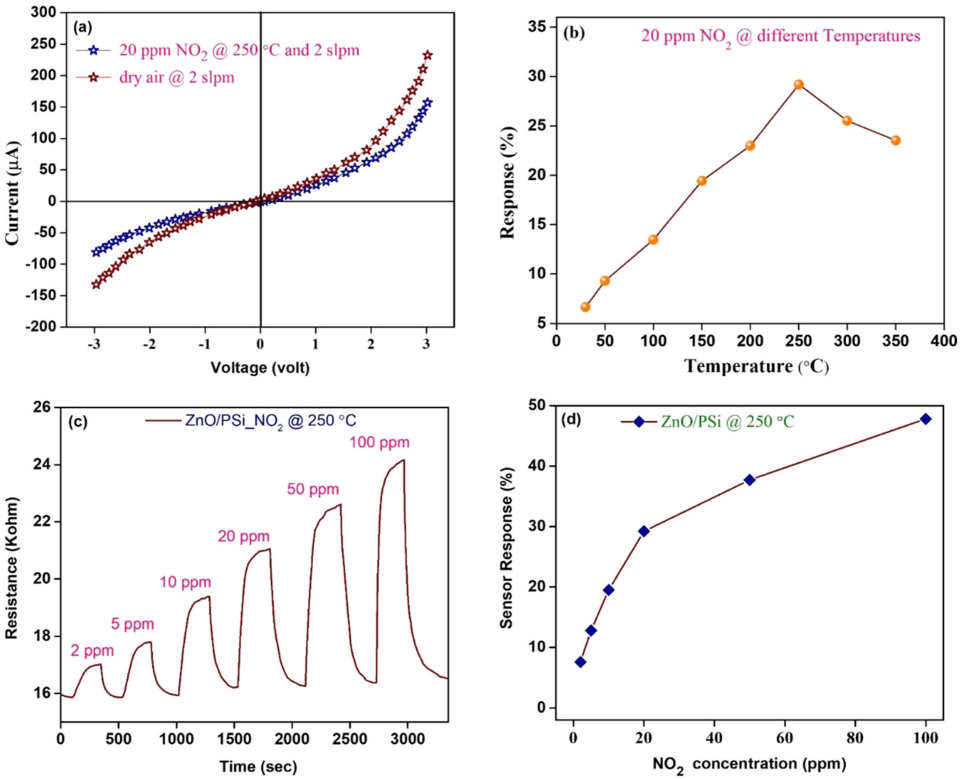

Figure 5: (a) I-V characteristics for ZnO/PSi thin film sample at 250°C in the presence of dry air and at 20 ppm NO_2 level, (b) Response versus temperature curve at different operating temperatures to 20 ppm NO_2, (c) Resistance versus time curve to different concentration (2 ppm–100 ppm) of NO_2 at 250°C for ZnO/PSi thin film sensor and (d) Sensor response versus NO_2 concentration curve at 250°C for ZnO/PSi sensor.

It can be observed due to slow chemical activation energy between the adsorbed analyte gas molecules and active sensing element at low operating temperatures. On the other hand, response starts to decline if temperature rises beyond 250°C. At high operating temperatures, desorption of analyte gas molecules occurs before the chemical reaction takes place.[27] The wide band

gap (3.2 eV) of ZnO corresponds to lower recombination rate of electron-hole pairs which caused to diminish the noise effect in the sensor signal. Thus, it can promote to synthesise the stable sensor signal even at high operating temperatures.[28]

Figure 5(c) depicts the sensor resistance versus time curve to different concentrations (2 ppm–100 ppm) of NO_2 at 250°C for ZnO/PSi thin film sensor. It revealed that the sensor response was progressively enhances as a function of the analyte gas concentration. Herein, we observed that the proposed sensor is able to detect trace amount of NO_2 down to 2 ppm at 250°C. The response time is defined as time lapsed to reach in 90% of maximum stable signal, and recovery time is defined as the time taken to recover the sensor signal up to 10% of the maximum stable value. Figure 5(d) shows the variation in the sensor response for ZnO/PSi sensor to different NO_2 concentrations (2 ppm–100 ppm) in dry air at flow rate of 2 slpm. During the sensing measurements, we controlled the flow of analyte gas mixed in dry air using mass flow controller (MFC). We have fixed the flow rate of dry air to 2 slpm and change the concentration of analyte gas at fixed flow rate to get the desired concentration. For chemiresistive gas sensors, the origin of sensor response is notable due to the interaction of analyte gas molecules on top surface of the sensitive layer. These outcomes show the noticeable rise in the sensor performance with enhancing the analyte gas concentration. The high sensing response can be documented to porous structure and large active surface area of ZnO/PSi sensor element.[28] It can be seen that such type of nanostructures may provide a path for fast transfer of charge carriers during the adsorption and desorption process of target gas molecules over the surface. The variation in sensing response with film thickness was also investigated in Figure S3. It reveals that the response to 20 ppm NO_2 at 250°C was observed to be maximum for 1.5 μm ZnO sensing layer. Initially the response gradually increases with thickness of sensing layer from 0.4 μm to 1.5 μm. Thereafter, the response started to decrease at higher thickness (2.2 μm) of ZnO layer. The decline in response at higher thickness of ZnO film might be due to the presence of microstructural defects in the sensing layer.[29] In addition, the sensor response could collaborate with the diffusivity of analyte gas molecules inside the sensing element. As a result, at higher thickness of ZnO layer, the response may start to decline due to the increase of the diffusion length for analyte gas molecules inside the sensing element.[30]

Figure 6(a) depicts the cyclability test for proposed sensor up to 6th cycles at 20 ppm NO_2 level in dry air. It shows that the response and recovery time was found to be 70 sec and 96 sec, respectively. It was observed that the ZnO/PSi

sensor exhibits almost stable signal up to 6th cycles, which collaborate to long term stability of the sensor chip for practical applications. Figure 6(b) shows the variation in response and recovery times with different concentrations of NO_2 at 250°C for ZnO/PSi nanoballs sensor. These results display the response time decreases with increasing the target gas concentration; however, the recovery time rises with enhancing the NO_2 concentration at 250°C. It can be recognised due to limited diffusion kinetics at lower concentrations of analyte gas molecules.[31] In addition, the high active surface area of ZnO nanoballs will provide the large number of catalytically improved surface reaction sites for significant adsorption of analyte gas, and hence enhanced the detection rate of NO_2.[7] Figure 6(c) displays the cross sensitivity test of ZnO/PSi nanoballs sensor at 20 ppm concentration of various gases. It can be seen that the proposed sensor device exhibits highest response (29.2%) to NO_2 with respect to weak response (13%) towards additional potentially interfering gases at 20 ppm level in dry air. It demonstrates that ZnO/PSi nanoballs sensor is highly selective to NO_2 gas in dry air at 250°C.

In this report, we developed hydrophobic thin films to prevent the effect of relative humidity on the sensor performance. To make the hydrophobic thin films firstly we developed the PSi substrates and then thin films were synthesised on these substrates which are prone to be hydrophobic. Thus, the effect of humidity on the sensor performance can be controlled by developing hydrophobic thin films for sensors operating at low temperature. Figure 6(d) reveals the sensor response versus humidity curve to 20 ppm NO_2 at 250°C. Here, we investigate the effect of humid environment on the sensor performance under different humidity conditions and about 8% decline in initial response was detected at 62% relative humidity conditions. The slightly drop in response is mostly attributed to the adsorption of hydroxyl ions (OH^-) on the sensor surface under high humid conditions. The decrease in sensor response in the presence of water molecules might be preventing the adsorption of target gas molecules on the sensor surface.[23] Therefore, the interaction of gas molecules with surface oxygen species may be deteriorated, which causes decrease in baseline resistance and hence declining the response.[32] In addition, the stability test of ZnO/PSi sensing element was performed to 20 ppm NO_2 in dry air up to four months at 250°C (Figure S4). It can be seen that about 7% change in the response signal was observed after four months. It is nearly constant response and exhibiting the long term stability of the proposed sensor. The change in the response value might be due to repeated heating of the active sensing element at 250°C.[33] Thus, the proposed sensing element possesses good quality life time for numerous practical applications. Brief summary of previous reported literature for ZnO based NO_2 gas sensor is shown in Table S1.

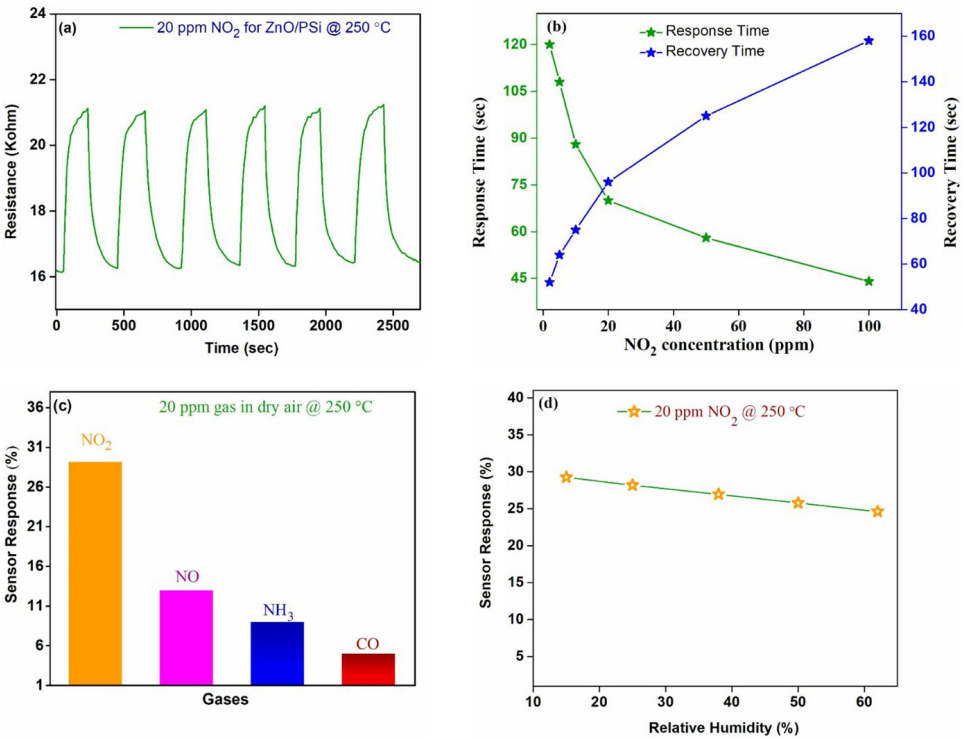

Figure 6: (a) The cyclability test up to 6th cycles at 20 ppm NO_2 level in dry air, (b) Shows the variation in response and recovery times with different concentrations (2 ppm–100 ppm) of NO_2 at 250°C for ZnO/PSi sensor, (c) Cross sensitivity test at 20 ppm concentration of various gases and (d) Depicts the response versus humidity curve at 20 ppm of NO_2 for proposed ZnO/PSi sensor.

3.3 Gas sensing mechanism

The gas sensing mechanism of chemiresistive based gas sensors depends on the change in electrical resistance upon adsorption and desorption of analyte gas molecules over the sensor surface. Metal oxide semiconducting materials adsorb the oxygen from environment and generate the different oxygen species (O_2^-, O^- and O^{2-}) at the top surface according to the operating temperature. The chemical reactions are gives as follow:

$$O_{2(gas)} + e^- \rightarrow O^-_{2(adsorbed)} \quad \text{for temperature less than 100°C} \tag{7}$$

$$O^-_{2(adsorbed)} + e^- \rightarrow 2O^-_{(adsorbed)} \quad \text{for temperature between 100°C to 300°C} \tag{8}$$

$$O^-_{(adsorbed)} + e^- \rightarrow O^{2-} \quad \text{for temperature greater than 300°C} \tag{9}$$

Basically, the carrier concentration of the sensing layer changes on reaction of target gas molecules with sensing material, which causes the change in electrical conductivity or resistance. Initially, oxide semiconducting electrode materials get adsorbed oxygen molecules from the ambient air and converted it into and oxygen species at the surface via following chemical reactions:

$$O_{2(gas)} \rightarrow 2O_{(adsorbed)} \tag{10}$$

$$O_{(adsorbed)} + e^-_{(from\ ZnO)} \rightarrow O^- \tag{11}$$

$$O_{(adsorbed)} + 2e^-_{(from\ ZnO)} \rightarrow O^{2-} \tag{12}$$

Equation (5) reveals that the electrons are extracted from the conduction band of sensing layer, which forms a surface depletion layer, resulting in decrease and increase the conductivity of n-type and p-type materials, respectively.

As we already know that NO_2 is an oxidising gas in nature which can react with the oxide surface directly or can react with sensing layer via adsorbed oxygen species present on the surface.[15, 34]

$$NO_2 + e^- \rightarrow NO_2^- \tag{13}$$

$$NO_2 + O^- + 2e^- \rightarrow NO_2^- + O^{2-} \tag{14}$$

$$NO_2 + O^{2-} + 2e^- \rightarrow NO_2^- + 2O^- \tag{15}$$

Here, higher electron affinity of NO_2 may extract a greater number of electrons from the oxide surface and hence electron concentration reduces which causes decline in conductivity for n-type sensing materials. However, in contrary, when the reducing gases interact with the n-type sensing layer, then reducing gas may donate its electrons to the sensing element which causes to enhance the conductivity.

4. CONCLUSIONS

In summary, we have synthesised a highly sensitive and selective NO_2 sensor based on PSi filled ZnO nanoballs using RF magnetron sputtering technique. Herein, all the sensing properties to NO_2 at low temperature were studied in detail. The proposed sensor depicts high sensing response (29.2%) with fast response and recovery time of 70 sec and 96 sec, respectively to 20 ppm of NO_2 gas in dry air at flow rate of 2 slpm. It also revealed the highly stable (up to four months) and reproducible (up to 6th cycles) sensor signal to 20 ppm NO_2 at

250°C. This sensor is capable to detect NO_2 down to 2 ppm at low operating temperature of 250°C. Thus, the PSi based thin film sensing device open up a novel approach to design a highly repeatable sensor with notable performance for low (ppm) detection of NO_2 in our environment at lower operating temperature regime.

5. ACKNOWLEDGEMENTS

Authors are thankful to the Department of Physics, Dr. Babasaheb Ambedkar Marathawada University, Aurangabad, Maharashtra, and would like to acknowledge the facilities and support provided to carry out the research work. We are also highly thankful to UGC special assistance programme.

6. REFERENCES

1. Manisalidis, I. et al. (2020). Environmental and health impacts of air pollution: A review. *Front. Public Health*. https://doi.org/10.3389/fpubh.2020.00014
2. Tollefson, J. (2010). Hydrogen vehicles: Fuel of the future. *Nature*, 464, 1262–1264. https://doi.org/10.1038/4641262a
3. Mazloomi, K. & Gomes, C. (2012). Hydrogen as an energy carrier: Prospects and challenges. *Renew. Sustain. Energy Rev.*, 16(5), 3024–3033. https://doi.org/10.1016/j.rser.2012.02.028
4. Chaulya, S. K. & Prasad, G. M. (2016). Gas sensors for underground mines and hazardous areas. In S. K. Chaulya (Ed.). *Sensing and monitoring technologies for mines and hazardous areas*. Netherlands: Elsevier, 161–212. https://doi.org/10.1016/B978-0-12-803194-0.00003-9
5. Peng, Y. et al. (2016). The hydrogen sensing properties of Pt–Pd/reduced graphene oxide based sensor under different operating conditions. *RSC Adv*., 6, 24880–24888. https://doi.org/10.1039/c5ra26618a
6. Khatibani, A. B. (2021). Investigation of gas sensing property of zinc oxide thin films deposited by Sol-Gel method: Effects of molarity and annealing temperature. *Indian J. Phys*, 95(2), 243–252. https://doi.org/10.1007/s12648-020-01689-4
7. Hariharan, V. et al. (2019). Role of chromium in tungsten oxide (WO_3) by microwave irradiation technique for sensor applications. *Indian J. Phys.*, 93, 459–465. https://doi.org/10.1007/s12648-018-1310-5
8. Fu, W. et al. (2017). Sensing at the surface of graphene field-effect transistors. *Adv. Mater*., 29(6), 1603610. https://doi.org/10.1002/adma.201603610
9. Sonker, R. K. et al. (2020). Synthesis of CdS nanoparticle by sol-gel method as low temperature NO_2 sensor. *Mater. Chem. and Phys.*, 239, 121975, https://doi.org/10.1016/j.matchemphys.2019.121975

10. Abbas, T. A. H. (2018). Light-enhanced vanadium pentoxide (V_2O_5) thin films for gas sensor applications. *J. Electron. Mater.*, 47, 7331–7342. https://doi.org/10.1007/s11664-018-6673-z
11. Kadhim, I. H. et al. (2016). Hydrogen gas sensor based on nanocrystalline SnO_2 thin film grown on bare Si substrates. *Nano-Micro Lett*., 8(1), 20–28. https://doi.org/10.1007/s40820-015-0057-1
12. Sun, Y. F. et al. (2012). Metal oxide nanostructures and their gas sensing properties: A review. *Sensors*, 12(3), 2610–2631. https://doi.org/10.3390/s120302610
13. Sonker, R. K. et al. (2019). Fabrication and characterization of ZnO-TiO_2-PANI (ZTP) micro/nanoballs for the detection of flammable and toxic gases. *J. Hazard. Mater.*, 370, 126–137. https://doi.org/10.1016/j.jhazmat.2018.10.016
14. Sonker, R. K. et al. (2018). Spherical growth of nanostructures ZnO based optical sensing and photovoltaic application. *Opt. Mater.*, 83, 342–347. https://doi.org/10.1016/j.optmat.2018.06.046
15. Sonker, R. K. & Yadav, B. C. (2017). Development of Fe_2O_3–PANI nanocomposite thin film based sensor for NO_2 detection. *J. Taiwan Inst. of Chemical Engineers*, 77, 276–281. https://doi.org/10.1016/j.jtice.2017.04.042
16. Sikarwar, S. et al. (2019). Synthesis and characterization of highly porous hexagonal shaped CeO_2-Gd_2O_3-CoO nanocomposite and its opto-electronic humidity sensing. *Appl. Surf. Sci.*, 479, 326–333. https://doi.org/10.1016/j.apsusc.2019.02.108
17. Quy, C. T. et al. (2017). Ethanol-sensing characteristics of nanostructured ZnO: Nanorods, nanowires, and porous nanoparticles. *J. Electron. Mater.*, 46, 3406–3411. https://doi.org/10.1007/s11664-016-5270-2
18. Sharma, D. et al. (2016). Sensitive measurement of nonlinear absorption and optical limiting in undoped and Fe-doped ZnO quantum dots using pulsed laser. *Indian J. Phys*., 90, 1293–1298. https://doi.org/10.1007/s12648-016-0837-6
19. Waikar, M. R. et al. (2020). Enhancement in NH_3 sensing performance of ZnO thin-film via gamma-irradiation. *J. Alloy. Compd*., 830, 154641. https://doi.org/10.1016/j.jallcom.2020.154641
20. Du, C. L. et al. (2006). Raman spectroscopy of (Mn, Co)-codoped ZnO films. *J. Appl. Phys.*, 99, 123515. https://doi.org/10.1063/1.2208298
21. Zhuo, R. F. et al. (2008). Morphology-controlled synthesis, growth mechanism, optical and microwave absorption properties of ZnO nanocombs. *J. Phys. D*: *Appl. Phys*., 41(18), 185405. https://doi.org/JPhysD/41/185405
22. Roach, P. et al. (2008). Progess in superhydrophobic surface development. *Soft Matter*, 4(2), 224–240. https://doi.org/10.1039/b712575p
23. Kim, K. S. & Chung, G. S. (2011). Characterization of porous cubic silicon carbide deposited with Pd and Pt nanoparticles as a hydrogen sensor. *Sens. Actuators B: Chem.* 157(2), 482–487. https://doi.org/10.1016/j.snb.2011.05.004
24. Wang, C. et al. (2010). Metal oxide gas sensors: Sensitivity and influencing factors. *Sensors*, 10(3), 2088–2106. https://doi.org/10.3390/s100302088

25. Donarelli, M. et al. (2016). Single metal oxide nanowire devices for ammonia and other gases detection in humid atmosphere. *Procedia Eng.*, 168, 1052–1055. https://doi.org/10.1016/j.proeng.2016.11.338
26. Wang, J. X. et al. (2009). N-P transition sensing behaviors of ZnO nanotubes exposed to NO_2 gas. *Nanotechnology*, 20, 465501. https://doi.org/10.1088/0957-4484/20/46/465501
27. Chen, J. et al. (2014). High-temperature hydrogen sensor based on platinum nanoparticle-decorated SiC nanowire device. *Sens. Actuators B Chem.*, 201, 402–406. https://doi.org/10.1016/j.snb.2014.04.068
28. Kim, K. S. et al. (2011). Characterization of porous cubic silicon carbide deposited with Pd and Pt nanoparticles as a hydrogen sensor. *Sens. Actuators B Chem.*, 157(2), 482–487. https://doi.org/10.1016/j.snb.2011.05.004
29. Hieu, N. V. et al. (2008). Highly sensitive thin film NH_3 gas sensor operating at room temperature based on SnO_2/MWCNTs composite. *Sens. Actuators B Chem.*, 129(2), 888–895. https://doi.org/10.1016/j.snb.2007.09.088
30. Sakai, G. N. et al. (2001). Theory of gas-diffusion controlled sensitivity for thin film semiconductor gas sensor. *Sens. Actuators B Chem.*, 80(2), 125–131. https://doi.org/10.1016/S0925-4005(01)00890-5
31. Choi, S. J. et al. (2016). Coaxial electrospinning of WO_3 nanotubes functionalized with bio-inspired Pd catalysts and their superior hydrogen sensing performance. *Nanoscale*, 8(17), 9159–9166. https://doi.org/10.1039/c5nr06611e
32. Sonker, R. K. et al. (2016). Experimental investigations on NO_2 sensing of pure ZnO and PANI–ZnO composite thin films. *RSC Adv.*, 6(61), 56149–56158. https://doi.org/10.1039/c6ra07103a
33. Guo, J. et al. (2014). High-performance gas sensor based on ZnO nanowires functionalized by Au nanoparticles. *Sens. Actuators B Chem.*, 199, 339–345. https://doi.org/10.1016/j.snb.2014.04.010
34. Mane, A. A. et al. (2016). Highly selective and sensitive response of 30.5% of sprayed molybdenum trioxide (MoO_3) nanobelts for nitrogen dioxide (NO_2) gas detection. *J. Colloid Interface Sci*., 483, 220–231. https://doi.org/10.1016/j.jcis. 2016.08.031